Journal of Chromatography, 355 (1986) 13–27
Elsevier Science Publishers B.V., Amsterdam — Printed in The Netherlands

CHROM. 18 298

ANALYTICAL AFFINITY CHROMATOGRAPHY

II. RATE THEORY AND THE MEASUREMENT OF BIOLOGICAL BINDING KINETICS

F. H. ARNOLD*,* and H. W. BLANCH
Department of Chemical Engineering, University of California, Berkeley, CA 94720 (U.S.A.)
(Received October 1st, 1985)

SUMMARY

Affinity chromatography can be used to measure equilibrium constants and kinetics of biological interactions. The local-equilibrium theory presented in the preceding paper is extended to include mass transfer and kinetic effects. Solutions for both zonal and frontal elution are presented. For highly nonlinear isotherms, the frontal elution method is preferred. Experiments with bovine serum albumin binding to immobilized Reactive Blue show that the binding kinetics inside the porous gel are several orders of magnitude slower than typical biological binding reactions in solution. The temperature dependence of the kinetic constants indicate that the binding may still be diffusion-controlled.

INTRODUCTION

In the preceding paper[1] we discussed analytical affinity chromatography as a method for measuring equilibrium constants for biological binding interactions. The retardation of a peak in zonal chromatography and the position of the breakthrough curve in frontal elution depend on the time the solute spends bound to the immobilized ligand as opposed to being carried along in the mobile phase. The degree to which the solute interacts with the ligand depends on the availability of binding sites and the strength of the solute–ligand interaction. The elution volume equations for both zonal and frontal chromatography each contain a term that is the product of the two, $\rho_B Q_{max} \cdot K_L$. Points on the equilibrium isotherm can be determined from the area behind the breakthrough curves at various values of the solute concentration c_0, as explained in the preceding paper[1]. A double-reciprocal plot of the isotherm then yields values for both K_L and $\rho_B Q_{max}$. The retardation of solute peaks in zonal elution, on the other hand, can give K_L only if $\rho_B Q_{max}$ has been measured independently, and *vice versa*.

* Current address: Department of Chemical Engineering, University of Minnesota, Minneapolis, MN 55455, U.S.A.

0021-9673/86/$03.50

In some situations, a set of experiments used to measure the equilibrium association constants can be extended in order to determine the binding kinetics as well. This can be done if the kinetics are sufficiently slow that they dominate the spreading of the peak or breakthrough curve. If the binding kinetics are slow and the resistance to mass transfer is minimized, it should be possible to obtain rate constants for the binding process from a careful investigation of the effluent concentration profiles.

Equilibrium constants can be measured either by zonal elution at low concentrations or by frontal elution over a wider range of concentration. Since the nonlinearity of the equilibrium isotherm has a relatively small effect on the exiting peak position, zonal elution can be used to measure equilibrium constants even for $K_L c_0 \approx 1$. Peak spreading, on the other hand, is a strong function of the local concentration. As a result, the measurement of kinetic constants by zonal elution must be performed and analyzed with this concentration dependence in mind. Up until now theories applied to zonal analytical affinity chromatography have not included nonequilibrium effects together with isotherm nonlinearity. In this paper we will discuss the applicable zonal and frontal elution models, extending the nonlinear theory presented in the previous paper to include nonequilibrium effects.

Muller and Carr[2] have used zonal affinity chromatography to determine the desorption rate constant for the binding of sugar derivatives to concanavalin A. They relied on the linear theory of Horváth and Lin[3] to interpret their experimental results. Hethcote and co-workers[4–6] have also considered analytical affinity chromatography as a method for measuring binding kinetics. Their approach to measuring kinetics is limited to linear equilibria, although they have considered the effects of isotherm nonlinearity on the average peak retention time[5]. Their single-component linear model is very similar to the chromatography theory developed by Kubin[7] and Kucera[8] and later extended by Smith and co-workers[9,10]. Hethcote and DeLisi[4] have also considered multivalent binding and competition from added soluble inhibitors. It has been shown[11] that the theory developed by Horváth and Lin[3] is identical to the earlier Kubin–Kucera theory. All of these theories rely on the use of the statistical moments to characterize the effluent profiles.

Chase[12,13] has recently published a series of papers on preparative affinity chromatography in which he used the nonlinear sorption rate-limited model of Hiester and Vermeulen[14] to predict breakthrough curves in frontal analysis. Using this approach Chase was able to study the binding of lysozyme and bovine serum albumin (BSA) to immobilized Cibacron blue and of β-galactosidase to immobilized antibodies. In contrast to the theories mentioned above, which predict the statistical moments, the Hiester–Vermeulen model leads to analytical expressions for the effluent solute concentrations at all times.

A feature common to the experimental studies mentioned above is the assumption that the rates of sorption are determined solely by the kinetics of the biological binding process, and not to, for example, slow diffusion of the solute into the porous particles. The kinetic constants thus measured are artificially small when the rate of mass transfer becomes comparable to the rate of binding. This assumption that the binding kinetics are rate-limiting does not come from limitations in the mathematical models, but rather from the difficulty in distinguishing binding kinetics from mass transfer in a single set of experiments. Once the mass transfer rate has

been determined in independent experiments or estimated from known diffusivities, the contribution to peak or breakthrough curve spreading can be included in the affinity chromatography model. This will be discussed further below when the equations for the concentration profiles are presented.

The Kubin–Kucera moment theory is limited to linear equilibria, and we have shown previously that extremely low concentrations are needed to fulfill this requirement for most biochemical kinetic studies[1]. This is true because significant peak spreading can occur when the equilibrium behavior becomes nonlinear, even in the limit of very fast kinetics. The Hiester–Vermeulen theory does not have this limitation. We will use the Hiester–Vermeulen model to determine binding kinetics by analytical affinity chromatography. Chase[12] has presented applications of the model in frontal analysis when the binding kinetics are rate-limiting. Here we will show how the model can be extended to include zonal elution as well as cases where mass transfer and sorption rates are comparable.

GOVERNING EQUATIONS

When extracting kinetic information from affinity experiments, the local equilibrium assumption can no longer be made. Instead, the possible rate-limiting steps in the sorption process must be explicitly included in the chromatography model. The governing equations are those presented in Part I[1] for local-equilibrium. To extend the model to cover departures from equilibrium, an equation to describe the finite adsorption and desorption rates is included. These equations have been discussed in greater detail in ref. 15*.

$$u_0 \frac{\partial c}{\partial z} + \varepsilon \frac{\partial c}{\partial t} + (1 - \varepsilon)\rho_p \frac{\partial q}{\partial t} = 0 \tag{1}$$

$$\frac{\partial q}{\partial t} = \mu_f c(Q_{max} - q) - \mu_r q \tag{2}$$

Eqn. 2, the binding rate equation, is second order in the forward direction and first order in the reverse direction, to correspond to interactions of the type

$$P + L \underset{\mu_r}{\overset{\mu_f}{\rightleftharpoons}} PL \qquad K_L = \frac{\mu_f}{\mu_r} = \frac{[PL]}{[P][L]} = \frac{q}{c(Q_{max} - q)}$$

This problem was first solved by Thomas[17] for frontal analysis and later by Goldstein[18] and Vermeulen *et al.*[19] for zonal elution. The frontal analysis result has been studied in detail by Hiester and Vermeulen[14], who extended it to include fluid- and particle-phase mass transfer as well as slow sorption kinetics.

---

* The equations reported by Chase[12], based on the review of fixed-bed adsorption models by Yang and Tsao[16], are not quite correct. Note also that the time t in Chase's papers is measured from the time at which non-adsorbing species exit the column, while t in this paper is measured starting from the time at which the feed is introduced to the front of the bed. The Chase definition is ambiguous since it depends on the size of the non-adsorbing species. If the solutes are too large to enter the pores, then the two times are related by $t(\text{Chase}) = t - \varepsilon L/u_0$. Eqn. 1 assumes that the rate of accumulation of solute in the pores of the affinity beads is small compared to $\rho_p \partial q/\partial t$, the rate of adsorption onto the particles.

To solve eqns. 1 and 2, it is convenient to use the following transformations proposed by Vermeulen and Hiester and discussed previously[15]:

$$X = \frac{c}{c_0} \qquad Y = \frac{q}{q_0} \qquad \text{where } q_0 = \frac{Q_{max} K_L c_0}{1 + K_L c_0} \tag{3}$$

$$N_{kin} = \frac{\mu_f(1 - \varepsilon)\rho_p Q_{max} L}{u_0}$$

$$R_{eq} = \frac{1}{1 + K_L c_0}$$

$$T = \frac{c_0}{(1 - \varepsilon)\rho_p q_0}\left(\frac{V - \varepsilon v}{v}\right) = \frac{c_0}{(1 - \varepsilon)\rho_p q_0}\left(\frac{u_0 t}{L} - \varepsilon\right)$$

The dimensionless group N is a "number of transfer units" for the column. L/N, or the "height of a transfer unit", is identical to the HETP (height equivalent to a theoretical plate) commonly found in the chromatography literature. When N is large, or the HETP is small, we are operating close to the local-equilibrium limit, and the peaks and breakthrough curves are sharp.

With these definitions, eqns. 1 and 2 become

$$\frac{\partial X}{\partial N} + \frac{\partial Y}{\partial NT} = 0 \tag{4}$$

$$\frac{\partial Y}{\partial NT} = X(1 - Y) - R_{eq} Y(1 - X) \tag{5}$$

Hiester and Vermeulen[14] have shown that it is also possible, with the appropriate transformation, to obtain eqn. 5 starting from the mass transfer equation with a linear concentration driving force:

$$(1 - \varepsilon)\rho_p \frac{\partial q}{\partial t} = K_{OL} a_p (c - c^*) \tag{6}$$

where c^* is the liquid concentration in equilibrium with the average concentration of bound material [$c^* = q/K_L(Q_{max} - q)$]. K_{OL} is the overall mass transfer coefficient, and a_p is the particle surface area per unit column volume. The product $K_{OL}a_p$ can be found from the peak spreading of unadsorbed tracers, as discussed in ref. 20. For mass transfer-limited sorption, the number of transfer units becomes

$$N_{m.t.} = \frac{2K_{OL} a_p L}{(R_{eq} + 1)u_0} \tag{7}$$

If the rate of mass transfer is comparable to the rate of the sorption step ($N_{m.t.} \approx N_{kin}$), then we can combine the processes as resistances in series and define an overall

number of transfer units:

$$N = \left[\frac{R_{eq} + 1}{2K_{OL}a_p} + \frac{1}{\mu_f(1 - \varepsilon)\rho_p Q_{max}}\right]^{-1} \frac{L}{u_0} \tag{8}$$

When affinity chromatography is used to investigate binding kinetics, it is important to design the experiment in such a way that the contributions to peak spreading from mass transfer and end effects do not overwhelm the kinetic contribution. In order for the mass transfer contribution to be small, the number of transfer units for mass transfer must be large compared to N for binding kinetics.

$$N_{m.t.} \gg N_{kin}$$

It is useful to estimate the observable rate constants for a particular system. Let us take the example of BSA binding to blue dye immobilized on Sepharose CL-4B. The overall rate of mass transfer is determined primarily by the slow diffusion of the large BSA molecules into the approximately 100-μm diameter particles. $K_{OL}a_p$ for this system has been measured from the second moments of BSA pulses on underivatized Sepharose CL-4B (0.034 s^{-1}) (ref. 20). The column we wish to use has a maximum binding capacity of $5 \cdot 10^{-5}$ M (3.3 mg/ml), and $K_L = 9 \cdot 10^5$ M^{-1}. If we choose a feed concentration such that $R_{eq} = 0.5$, then

$$\mu_f < \frac{2(0.034)}{1.5(5 \cdot 10^{-5})} \approx 10^3 \; M^{-1} \; s^{-1}$$

The experiments will be able to measure the forward rate constant only if it is smaller than about 10^3 M^{-1} s^{-1}, which is two to three orders of magnitude smaller than forward rate constants commonly measured for biological interactions in solution.

The situation can be improved somewhat by decreasing the mass transfer resistance. This is most easily done by using smaller beads. A reduction in the particle size by a factor of three will decrease the overall mass transfer coefficient by roughly a factor of $3^2 = 9$, which leads to an order-of-magnitude extension in the measurable μ_f. At a certain point, however, the mass transfer resistance will be decreased so much that other dispersive mechanisms such as mixing in the distributor and detector will dominate the peak spreading. Hethcote and DeLisi[6] have proposed reducing the mass transfer contribution by immobilizing the macromolecular species and allowing the small molecule to diffuse to the binding sites. This does not work, of course, if the solute and ligand are both macromolecules. A significant disadvantage of their scheme is the difficulty of detecting equivalent molar concentrations of small molecules.

SOLUTIONS

Zonal elution

For a pulse of duration t_0, we can define a dimensionless pulse time T_0 as

$$T_0 = \left[\frac{c_0}{(1 - \varepsilon)\rho_p q_0}\right] \frac{u_0 t_0}{L} \tag{9}$$

The exiting concentration profile, X as a function of T for a given pulse T_0, depends only on the two parameters R_{eq} and N. The solution to eqns. 4 and 5 for a finite pulse is[18]

$$X = \frac{J(R_{eq}N,NT) - J(R_{eq}N,NT - NT_0)}{P} \qquad (R_{eq} \leqslant 1) \tag{10}$$

where

$$P = \exp\{(1 - R_{eq})(N - NT)\}[1 - J(N,R_{eq}NT)] +$$

$$+ J(R_{eq}N,NT) - J(R_{eq}N,NT - NT_0) +$$

$$+ \exp\{(1 - R_{eq})(N - NT + NT_0)\}J(N,R_{eq}NT - R_{eq}NT_0)$$

Evaluation of the J function is discussed in the Appendix.

Eqn. 10 can be used to illustrate how nonlinearity in the equilibrium isotherm affects the shape and position of an exiting peak. As the concentration of the sample pulse is increased, R_{eq} becomes smaller. The peaks exit earlier since a given solute molecule has fewer encounters with immobilized ligands. Furthermore, the peaks are no longer symmetrical as they are for very small concentrations, where $R_{eq} = 1$. This loss of symmetry has been seen in the peaks predicted by local-equilibrium theory[1].

Dispersion opposes this effect by lowering the local concentrations so that they have velocities that are more similar. Therefore dispersion acts to smooth out the sharp boundaries in the chromatograms shown in the previous paper for nonlinear local equilibrium theory. The effects of increasing the sample concentration are illustrated in Fig. 1: increasing c_0 causes a decrease in the average retention time and greater asymmetry of the peaks. It is difficult to calculate the second moments of peaks with large degrees of tailing since small changes in the baseline lead to large errors in higher order statistical moments.

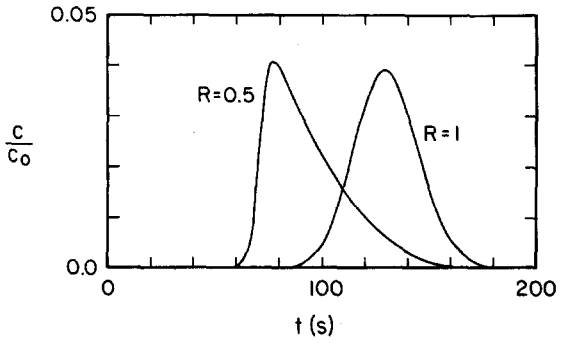

Fig. 1. Elution profiles in zonal chromatography with nonlinear equilibrium. Increasing the concentration in the pulse decreases the retention time and increases tailing. Values used in the calculation: $L = 5$ cm; $u_0 = 0.236$ cm s^{-1}; $\varepsilon = 0.80$; $t_0 = 1.5$ s; $\mu_r = 0.1$ s^{-1}; $K_L = 1.6 \cdot 10^4\ M^{-1}$; $\rho_B Q_{max} = 3.31 \cdot 10^{-4}\ M$.

In the limit of linear equilibria ($R_{eq} = 1$), eqn. 10 simplifies to

$$X = J(N,NT) - J(N,NT - NT_0) \qquad (R_{eq} = 1) \tag{11}$$

This solution can be used to predict elution profiles for preparative gel filtration chromatography with large pulses that may or may not be resolved at the column exit. The Kubin–Kucera/Smith and the Hethcote–DeLisi theories for zonal elution are limited to predicting the statistical moments of the exiting peak. Since the solutions presented here give the whole concentration profile, they are particularly useful when one wishes to calculate product recovery or dilution in preparative-scale chromatography. Eqn. 11 and the Kubin–Kucera theory give identical numerical values for the peak moments.

Frontal elution

Eqn. 12 predicts the breakthrough profile that would be expected from an affinity column when the solute is fed continuously starting at time $t = 0$. This solution shows that the exiting concentration for a given column as a function of effluent volume depends solely on the equilibrium parameter R_{eq} and the number of transfer units for the column. The definitions of R_{eq} and N are the same as before: the column and interactions that lead to peak spreading and retention are the same ones that determine the breakthrough behavior. Only the boundary conditions are different.

$$X = \frac{J(R_{eq}N,NT)}{J(R_{eq}N,NT) + \exp\{(R_{eq} - 1)(NT - N)\}[1 - J(N,R_{eq}NT)]} \tag{12}$$

$(R_{eq} \leqslant 1)$

EXPERIMENTAL METHODS

The adsorption of BSA (Sigma, crystallized and lyophilized) onto an immobilized blue triazine dye (Reactive Blue, Sigma) was studied by frontal elution chromatography to exemplify the use of the preceding theory. Immobilized blue dye is widely used to purify NAD-dependent enzymes and plasma proteins. The interaction of the dye molecule with BSA appears to involve more than one binding site on the protein[21]. The Reactive Blue was immobilized onto Sepharose CL-4B and Superose CL-6B (Pharmacia) using the procedure of Dean and Quadri[21]. A relatively small amount of Reactive Blue was coupled to the gels in order to keep the BSA binding capacity low (*ca.* 4 mg/ml) for these experiments. The experiments described below were performed on gels prepared in single batches. No loss of capacity was detected after repeated use.

Breakthrough curves were recorded at several temperatures for a range of feed concentrations and residence times (L/u_0) in order to measure the equilibrium association constants and to identify the rate-limiting step in the binding process. The apparatus used to detect the breakthrough curves consisted of an Altex 153 spectrophotometer connected to an HP 3421 data logger and HP 85 computer/controller.

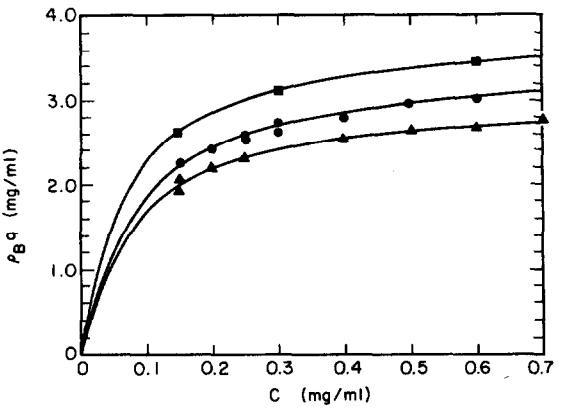

Fig. 2. Equilibrium isotherms obtained from breakthrough curves of bovine serum albumin binding to Reactive Blue–Sepharose CL-4B. ▲, 5°C; ●, 30°C; ■, 47°C.

RESULTS

Equilibrium

The area behind the breakthrough curve corresponds to the equilibrium capacity of the affinity gel at the feed concentration used. Thus the isotherm can be generated by integrating the breakthrough curves for different c_0. Isotherms were generated in this way for BSA binding to Blue-Sepharose CL-4B at 5, 15, 30 and 47°C. Three of the isotherms are shown in Fig. 2. (The data at 15°C have been omitted for clarity.) The solid lines correspond to the Langmuir isotherms that best fit the data in a double-reciprocal plot ($1/\rho_B q$ *vs.* $1/c_0$). The association constants and maximum binding capacities are listed in Table I for the four temperatures.

Although there is no clear trend in the values of the equilibrium binding constants K_L, the apparent maximum capacity $\rho_B Q_{max}$ increases as the temperature is increased from 5 to 47°C. This could be caused by swelling of the gel at higher temperatures, making more binding sites available in the interior of the beads. The increase could also be due to deviations from the Langmuir-type equilibrium behavior in which every site is equivalent. This is quite possible since the binding of BSA to the blue dye is somewhat non-specific and there is apparently more than one dye

TABLE I

EQUILIBRIUM BINDING RESULTS FOR BSA ADSORBING ONTO REACTIVE BLUE–SEPHAROSE CL-4B

		Temperature (°C)			
		5	*15*	*30*	*47*
$\rho_B Q_{max}$	(mg/ml)	3.06	3.12	3.43	3.88
$\rho_B Q_{max}$	(M)	$4.6 \cdot 10^{-5}$	$4.7 \cdot 10^{-5}$	$5.2 \cdot 10^{-5}$	$5.9 \cdot 10^{-5}$
K_L	(M^{-1})	$8.1 \cdot 10^5$	$7.6 \cdot 10^5$	$7.7 \cdot 10^5$	$9.0 \cdot 10^5$

binding site per BSA molecule. However, the data in Fig. 2 are described very well by the Langmuir equation.

The binding of BSA to the dye results from a combination of electrostatic and hydrophobic interactions[21]. The hydrophobic interactions are largely entropic in nature, while the electrostatic interactions contribute to the enthalpy. The overall free energy change ΔG associated with binding may have a rather complex temperature dependence since $\Delta G = \Delta H - T\Delta S$.

Kinetics

Once the equilibrium binding constant has been determined, the separation factor R_{eq} can be evaluated. The experimental breakthrough curves can then be compared to those predicted by eqn. 12 in order to estimate the number of transfer units, N, for the affinity adsorption. By studying the variation of N with flow-rate, temperature, and particle size, it should be possible to identify and quantify the rate-determining step in the affinity adsorption. The binding rate constant can be measured in this way, providing it is sufficiently small. In order to do this one must first estimate the contribution to the shape of the breakthrough profile that arises from the slow diffusion of the solute into the particles.

The overall mass transfer coefficients for BSA diffusing into particles of Sepharose CL-4B has been measured at 21°C by zonal elution chromatography on underivatized gel[15]. In order to estimate $K_{OL}a_p$ for the four different temperatures, it has been assumed that K_{OL} is proportional to the diffusivity, which depends directly on temperature and indirectly through the viscosity of the surrounding medium. From the Stokes–Einstein relationship, $D \propto \mu/T$ (K). Using the temperature dependence of the viscosity of water and the value of $K_{OL}a_p$ measured at 21°C, the following values for the overall mass transfer coefficient have been estimated at the various temperatures.

Temperature (°C):	5	15	(21)	30	47
$K_{OL}a_p$ (s^{-1}):	0.021	0.028	(0.034)	0.043	0.063

If the actual binding of the BSA to the immobilized dye was fast compared to the diffusion of the protein into the particles, the value of N for the adsorption breakthrough curve would be given by eqn. 7, using the values of $K_{OL}a_p$ listed above.

Typical breakthrough curves are shown in Fig. 3. The experimental curves are represented by the circles, while the profiles predicted by eqn. 11 that best fit the slope of the experimental curve at the midpoint ($c = 0.5c_0$) are represented by the lines. Both profiles were generated at approximately the same feed concentration and residence time; the difference in the curves reflects the effect of temperature on the rate of diffusion and binding.

The values of N predicted by eqn. 7 for adsorption that is limited only by the rate of mass transfer into the particles would be $N = 127$ at 30°C and $N = 60$ at 5°C for the conditions of the experiment in Fig. 2. The N values found from the actual breakthrough curves are considerably smaller, which indicates that, in addition to diffusion, there is another slow step in the adsorption of BSA onto the dye immobilized in the macroporous particles.

Data for a number of breakthrough curves at 5°C are presented in Table II.

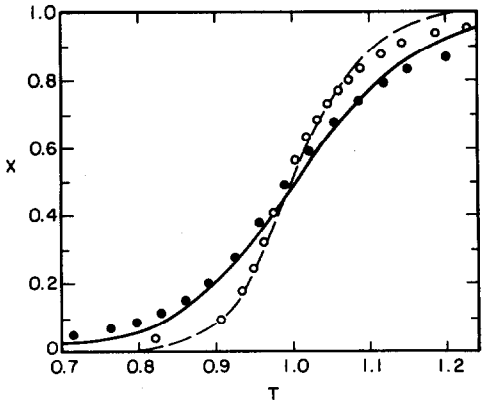

Fig. 3. Breakthrough curves for bovine serum albumin binding to Reactive Blue–Sepharose CL-4B. c_0 = 0.6 mg/ml. ●, 5°C, L/u_0 = 1580 s, N = 15; ○, 30°C, L/u_0 = 1660 s, N = 26.

TABLE II

RESULTS FROM BREAKTHROUGH CURVES FOR BSA ADSORBING ONTO SEPHAROSE CL-4B–REACTIVE BLUE AT 5°C

Feed conc. c_0 *(mg/ml)*	N	L/u_0 *(s)*	$\frac{N}{(L/u_0)}$ (s^{-1})	μ_f $(M^{-1}\,s^{-1})$
0.15	20	1700	0.012	410
0.15	15	1570	0.010	297
0.20	18	1620	0.011	370
0.25	21	2380	0.009	260
0.40	21	2600	0.008	226
0.50	17	1730	0.010	290
0.60	15	1580	0.009	277
0.70	15	1510	0.010	291

TABLE III

BINDING RATE CONSTANTS MEASURED BY ANALYTICAL AFFINITY CHROMATOGRAPHY

BSA binding to immobilized Reactive Blue.

Temperature (°C)	μ_f $(M^{-1}\,s^{-1})$
5	3.0 ± 1*
15	3.9 ± 1
30	5.5 ± 1.5
47	(5)

* Values ± standard deviation.

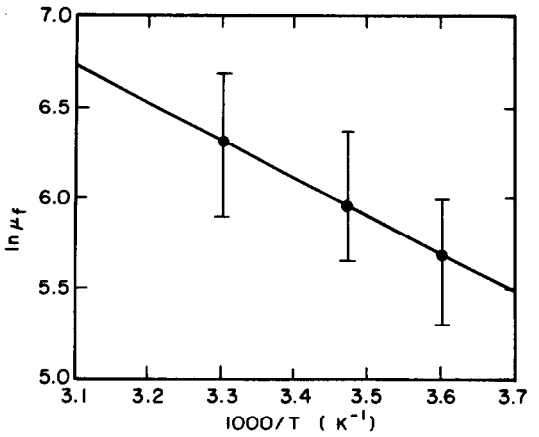

Fig. 4. Temperature dependence of forward binding rate constant for bovine serum albumin on Reactive Blue–Sepharose CL-4B. Error bars indicate spread of measured values.

The contribution of mass transfer to the overall number of transfer units can be calculated from the known feed concentration and $K_{OL}a_p$ for this temperature. The binding rate constant can then be calculated using eqn. 8. The results are summarized in Table III for the four temperatures. Each value of μ_f is based on at least eight separate measurements, except for the point at 47°C, which is based on only two.

A plot of ln μ_f *versus* $1/T$ is presented in Fig. 4. Only the points at 5, 15 and 30°C have been included. If the forward rate constant is described by an Arrhenius equation,

$$\mu_f = A \exp[-E_a/RT] \tag{13}$$

one obtains the activation energy $E_a = 4$ kcal mole^{-1} and the preexponential factor $A = 4.4 \cdot 10^5\ M^{-1}\ s^{-1}$. The temperature coefficient is small, within experimental error of the temperature coefficient of the viscosity of liquid water ($E_a = 3$ kcal mol^{-1}), expected for a diffusion-controlled reaction.

In order to study the effect of particle size on the breakthrough behavior, several breakthrough curves were measured on an adsorbent made by immobilizing the Reactive Blue on Superose CL-6B. Superose is an agarose-based gel similar to Sepharose, but with a mean particle size of 30 μm. The overall mass transfer coefficient for BSA diffusing into this gel was measured and found to be 0.12 s^{-1}, or about three times greater than the $K_{OL}a_p$ in Sepharose. This increase in the mass transfer coefficient is less than would be expected from the roughly three-fold reduction in the particle size. However, the Superose is a denser matrix than Sepharose (6% *vs.* 4%) and probably has smaller, more tortuous pores[15]. The results from the breakthrough experiments on Blue-Superose are summarized in Table IV.

If the adsorption process were limited only by the solute diffusion, then much sharper breakthrough profiles would be expected from the Superose beds. However, the overall adsorption rate (Nu_0/L) measured for Superose is actually less than that on Sepharose at the same temperature. Therefore, the rate-limiting step cannot be

TABLE IV
RESULTS OF BREAKTHROUGH EXPERIMENTS ON REACTIVE BLUE–SUPEROSE CL-6B AT 21°C

$\rho_B Q_{max}$ = 6.5 mg/ml (BSA) = $9.8 \cdot 10^{-5}$ M; $K_L = 1.3 \cdot 10^6$ M^{-1}; $K_{OL} a_p = 0.12$ s^{-1}.

c_0 (mg/ml)	N	$\frac{N}{L/u_0}$ (s^{-1})	μ_f (M^{-1} s^{-1})
0.4	15	0.012	128
0.5	12	0.009	97
0.6	15	0.012	131
0.8	15	0.012	132
1.0	15	0.012	123
		Average:	122

simply the diffusion of solute into the pores. The results are consistent instead with an adsorption mechanism that is kinetic rather than diffusion limited.

DISCUSSION

The forward binding constant obtained for the BSA binding to reactive blue in the Superose gel is smaller than the rate constant in Sepharose (440 M^{-1} s^{-1}). It is possible that the degree of protein already bound to the matrix affects binding kinetics via steric hindrance at the binding sites or pore entrances. The Superose gel used in these experiments had about twice the capacity of the Sepharose. The capacities of the adsorbents used in these experiments, however, is much smaller than the maximum attainable capacities (*ca.* 20 mg/ml). The gels were made with low capacities in order to minimize the effects of steric hindrance due to high loading. The effects of loading on kinetics were not investigated.

The binding rate constants measured in this study are considerably smaller than rate constants characteristic of diffusion-controlled biological reactions in solution. The source of this slow binding of the protein to the immobilized ligand is not clear. It is possible that the presence of the surface next to the ligand makes it difficult for the large albumin molecule to approach at a proper orientation for binding. Or, perhaps, the presence of the gel matrix hinders the rotation of the protein as well as the translational motion. It is possible that this reaction is still diffusion limited, with additional constraints imposed by the pore surfaces. This might explain the smaller rate constant measured in Superose beads. Another possibility is that the small dye molecule interacts with the surface in such a way that only a fraction of the ligands are available for binding at any given instant. A collision between the protein and such a sequestered ligand would not lead to binding.

CONCLUSIONS

The frontal elution technique is preferred to zonal elution for measuring the kinetics of strongly interacting biological molecules. Zonal methods have relied on the assumption of a linear equilibrium isotherm, an assumption that is unjustified for most biological systems. A theory for nonlinear zonal elution has been presented.

The chromatography theories presented here allow one to separate the effects of mass transfer from binding kinetics provided the overall mass transfer coefficient for the system is known. Overall mass transfer coefficients can be measured by zonal chromatography, as discussed in ref. 15.

The forward binding rate constant measured for BSA interacting with immobilized blue dye is three orders of magnitude smaller than rate constants of diffusion-controlled biological binding reactions in solution. The temperature dependence of the binding kinetics, however, is consistent with diffusion control. The activation energy is approximately 4 kcal/mole. It is possible that the low rate constant reflects the macromolecule's difficulty in finding the proper orientation for binding within the confined spaces of the pores.

ACKNOWLEDGEMENTS

The authors wish to thank Jack Hwang for his helpful contributions to this work. This research was funded by the Center for Biotechnology Research, San Francisco, CA.

APPENDIX

Evaluation of the J function

Accurate evaluation of J is critical for the zonal elution solution (eqn. 9). The J function is defined as

$$J(x,y) = 1 - \exp(-y)\int_0^x \exp(-\tau) I_0(2\sqrt{\tau y})\,d\tau$$

In order to calculate J, we have made use of the following equalities[18]

$$J(x,y) = e^{-(x+y)} \sum_{m=0}^{\infty} \eta^m I_m(\zeta) = 1 - e^{-(x+y)} \sum_{m=1}^{\infty} \eta^{-m} I_m(\zeta)$$

where

$$\zeta = 2\sqrt{xy} \qquad \eta = \sqrt{y/x}$$

I_m is the modified Bessel function of mth order. To find I_m, it is convenient to use the recurrence relation for Bessel functions:

$$I_{m+1}(x) = I_{m-1}(x) - \frac{2m}{x} I_m(x)$$

Because of the numerical instability of this relationship, errors in succeeding calculations increase rapidly. Only five terms were calculated in this way before obtaining new values from the infinite series.

The major difficulties encountered in the calculation of the concentration profile were: (1) the overflow of exponents in the denominator of eqn. 9 and (2) evaluating the numerator when the values of the two J functions were very similar. The latter problem was solved by using the Taylor series expansion of the J function about 1 and then subtracting the two series. The overflow problem was solved by absorbing the exponent $\exp(-R-NT)$ into the series and then taking the logarithm of each term.

For values of x and y such that $(xy)^{\frac{1}{2}} \geqslant 7$, the following (Onsager) approximation can be used:

$$J(x,y) = \frac{1}{2}\left\{1 - \operatorname{erf}(\sqrt{x} - \sqrt{y}) + \frac{\exp[-(\sqrt{x} - \sqrt{y})^2]}{\sqrt{\pi}[\sqrt{y} + \sqrt[4]{xy}]}\right\}$$

SYMBOLS

a_p particle surface area per unit volume (cm^{-1})
c bulk liquid concentration (M)
c_i average solute concentration in pore liquid (M)
c_0 feed or pulse concentration (M)
q average sorbate concentration (mmoles g^{-1} particle)
t time elapsed from injection of sample (s)
t_0 pulse length (s)
u_0 liquid superficial velocity (cm s^{-1})
v total column volume (cm^3)
z distance along column (cm)
A column cross section (cm^2)
K_L Langmuir or association constant (M^{-1})
K_{OL} overall mass transfer coefficient (cm s^{-1})
L column length (cm)
N dimensionless number of transfer units
Q_{max} maximum number of available sites (mmoles g^{-1} particle)
R dimensionless separation factor
T dimensionless effluent volume
V effluent volume ($= u_0At$) (cm^3)
X dimensionless solute concentration
Y dimensionless sorbate concentration
β particle volume fraction available to solute
ε column void fraction
μ viscosity
μ_1 average retention time (s)
μ_f forward binding rate constant (M^{-1} s^{-1})
μ_r reverse binding rate constant (s^{-1})
ρ_B bulk density [$= \rho_p(1 - \varepsilon)$] (g cm^{-3} particle)
ρ_p particle density (g cm^{-3} particle)

REFERENCES

1 F. H. Arnold, S. A. Schofield and H. W. Blanch, *J. Chromatogr.*, 355 (1986) 1.
2 A. J. Muller and P. W. Carr, *J. Chromatogr.*, 284 (1984) 33.
3 Cs. Horváth and H.-J. Lin, *J. Chromatogr.*, 149 (1978) 43.
4 H. W. Hethcote and C. DeLisi, *J. Chromatogr.*, 248 (1982) 183.
5 C. DeLisi, H. W. Hethcote and J. W. Brettler, *J. Chromatogr.*, 240 (1982) 283.
6 H. W. Hethcote and C. DeLisi, in I. M. Chaiken, M. Wilchek and I. Parikh (Editors), *Affinity Chromatography and Biological Recognition*, Academic Press, Orlando, FL, 1983, p. 119.
7 M. Kubin, *Collect. Czech. Chem. Commun.*, 30 (1965) 1104.
8 E. Kučera, *J. Chromatogr.*, 19 (1965) 237.
9 M. Suzuki and J. M. Smith, *Chem. Eng. Sci.*, 26 (1971) 221.
10 T. Furusawa, M. Suzuki and J. M. Smith, *Catal. Rev.-Sci. Eng.*, 13 (1976) 43.
11 F. H. Arnold, H. W. Blanch and C. R. Wilke, *J. Chromatogr.*, 330 (1985) 159.
12 H. A. Chase, *J. Chromatogr.*, 297 (1984) 179.
13 H. A. Chase, *Chem. Eng. Sci.*, 39 (1984) 1099.
14 N. K. Hiester and T. Vermeulen, *Chem. Eng. Prog.*, 48 (1952) 505.
15 F. H. Arnold, H. W. Blanch and C. R. Wilke, *Chem. Eng. J.*, 30 (1985) B9.
16 C.-M. Yang and G. T. Tsao, *Adv. Biochem. Eng.*, 25 (1982) 1.
17 H. C. Thomas, *J. Phys. Chem.*, 66 (1944) 1664.
18 S. Goldstein, *Proc. R. Soc., Ser. A*, 219 (1953) 151.
19 T. Vermeulen, G. S. Klein and N. K. Hiester, in R. H. Perry and C. H. Chilton (Editors), *Chemical Engineer's Handbook*, McGraw-Hill, NY, 1983.
20 F. H. Arnold, H. W. Blanch and C. R. Wilke, *Chem. Eng. J.*, 30 (1985) B25.
21 P. D. Dean and F. Quadri, *Chem. Anal.*, 66 (1983) 79.